Journal of Zhejiang University SCIENCE A
ISSN 1673-565X (Print); ISSN 1862-1775 (Online)
www.zju.edu.cn/jzus; www.springerlink.com
E-mail: jzus@zju.edu.cn

***Review:***

# *J*-integral resistance curve testing and evaluation

Xian-kui ZHU
(*Battelle Memorial Institute, Columbus, Ohio 43221, USA*)
E-mail: zhux@battelle.org

Received July 27, 2009; Revision accepted July 31, 2009; Crosschecked Aug. 7, 2009

**Abstract:** In this paper a critical review is presented of the history and current state of the art of *J*-integral resistance curve testing and experimental evaluation methods in conjunction with a discussion of the development of the plane strain fracture toughness test standard ASTM E1820 developed by American Society for Testing and Materials (ASTM). Early research efforts on this topic are reviewed first. These include the *J*-integral concept, experimental estimates of the *J*-integral for stationary cracks, load line displacement (LLD) and crack mouth opening displacement (CMOD) based $\eta$ factor equations, different formulations of *J*-integral incremental equations for growing cracks, crack growth corrected *J*-*R* curve determination, and experimental test methods. Recent developments in *J*-*R* curve testing and evaluation are then described, with emphasis on accurate *J*-integral incremental equations, a normalization method, a modified basic method, a CMOD direct method with use of incremental equations, relationships of plastic geometry factors, constraint-dependent *J*-*R* curve testing and correction approaches. An overview of the present fracture toughness test standard ASTM E1820-08a is then presented. The review shows that after more than 40 years of investigation and development, the *J*-integral resistance curve test methods in ASTM E1820 have become simpler, more cost-effective and more accurate.

**Key words:** *J*-integral, *J*-*R* curve, Fracture toughness, Fracture testing, Crack growth
**doi:**10.1631/jzus.A0930004 **Document code:** A **CLC number:** TB3

## INTRODUCTION

Fracture toughness is a material property which describes the ability of a material containing a crack to resist fracture. For brittle fracture, the toughness is often measured as a point value and is characterized by the stress intensity factor *K* that is used for linear elastic materials. For ductile fracture, the toughness can be measured as a point value or in a resistance curve format and is often characterized by the *J*-integral that is used for elastic-plastic materials. Usually, a *J*-integral based resistance curve (i.e., a *J*-*R* curve) is used to describe a ductile material's resistance against crack initiation, stable growth and tearing instability. Because of their effectiveness in measuring toughness, the *J*-integral and *J*-*R* curve have become the most important material parameters in elastic-plastic fracture mechanics, and have been applied widely in practical engineering. Such fracture toughness values may serve as a basis for material characterization, performance evaluation, and quality assurance. They can also be used for structural damage tolerance assessment, fitness-for-service evaluation, residual strength analysis and structural integrity management for various engineering components and structures, such as pressure vessels and piping in nuclear power plants, petrochemical vessels and tanks, onshore and offshore pipelines in oil and gas industries, and aircraft structures.

The theoretical *J*-integral concept was proposed by Rice (1968) and was used originally as a measure of the intensity of elastic-plastic crack-tip fields. The pioneering experimental work of Begley and Landes (1972) made the *J*-integral become a measurable material parameter. Since then, extensive analytical, numerical and experimental investigations have been conducted in development of effective test methodologies for evaluating a critical *J*-integral for stationary cracks and a *J*-*R* curve for growing cracks. Some early overviews of this topic can be found in (Turner, 1981; 1983; Kanninen and Popelar, 1985; Anderson, 1995). Detailed experimental techniques

and test procedures for *J*-*R* curve testing have been developed in the USA by the American Society for Testing and Materials (ASTM), as documented in an ASTM manual authored by Joyce (1996). In the first *J*-based fracture toughness test standard ASTM E813, issued in 1981, only the experimental result of the critical *J*-integral at the onset of ductile tearing was accepted as a measure of the fracture toughness of materials. The later versions, including ASTM E1152, E1737 and E1820, provided the standard test procedures and methods for critical *J* and *J*-*R* curve testing.

ASTM E1820 is a worldwide standard for measuring critical *J*-integral and *J*-*R* curves. The recommended specimens are single edge-notched bend (SENB or SE(B)), compact tension (CT), and disk-shaped compact tension (DCT) specimens. The recommended test procedure is an elastic unloading compliance method for measures of multiple data points from a single specimen. It requires continuous measurements of applied load, load-line displacement (LLD) and crack mouth opening displacement (CMOD). The test data are used to determine specimen compliance, instantaneous crack length and *J*-integral values for a growing crack. The *J*-integral values are calculated from an LLD-based incremental equation proposed by Ernst *et al*.(1981). A *J*-*R* curve is then obtained as the *J*-integral plotted against crack extension, which exhibits increasing fracture toughness as the crack grows. However, heavy data acquisitions plus complicated test procedures made the *J*-*R* curve testing very expensive and time-consuming. Therefore, much time and effort has been devoted to simplifying test procedures and reducing test costs. Alternative, cost-effective approaches and technologies were then developed including the normalization method standardized by Joyce (2001) and the CMOD direct method proposed by Zhu *et al*.(2008). These methods have significantly improved the ASTM standard test procedures for *J*-*R* curve testing.

A detailed review of *J*-integral resistance curve testing and evaluation is provided in this paper with emphasis on recent developments. The following sections first introduce the *J*-integral estimate and test methods for both stationary and growing cracks using LLD and CMOD data. Recent developments are then described with a focus on accurate *J*-integral incremental equation, a normalization method, a modified basic method, a CMOD direct method, plastic geometry factor determination and constraint-dependent *J*-*R* curve formulation. An overview is then given of the fracture toughness test methods recommended in the present ASTM standard E1820-08a.

## EXPERIMENTAL ESTIMATES AND TEST METHODS OF *J*-INTEGRAL

### *J*-integral estimates for stationary cracks

Originally, Rice (1968) proposed a path independent *J*-integral based on the deformation theory of plasticity. This was used as a loading parameter to measure the crack-tip singularity intensity of the HRR field (Hutchinson, 1968; Rice and Rosengren, 1968) for elastic-plastic hardening materials. Broad finite element analyses showed that HRR solutions can reasonably match the crack-tip fields for deeply cracked bending specimens, and that the *J*-integral can well describe the stresses, strains and other mechanics behaviors at the crack tip. So motivated, extensive experimental investigations on *J*-integral testing were then conducted with the aim of developing effective test methods for evaluating its value. Among the pioneers, Begley and Landes (1972) and Landes and Begley (1972) first successfully measured the *J*-integral and its critical value using multiple laboratory-scale specimens with mode-I tensile cracks. Since then, the *J*-integral has become a measurable material parameter for characterizing the fracture toughness of ductile materials.

In the early experimental evaluation, the *J*-integral was interpreted as a strain energy release rate, or work done to the specimen per unit fracture surface area in a material given by

$$J = -\frac{1}{B}\frac{\mathrm{d}U}{\mathrm{d}a}, \tag{1}$$

where $U$ is strain energy, $a$ is crack length and $B$ is specimen thickness. Begley and Landes (1972) tested a series of fracture specimens of the same geometry with different crack sizes and instrumented load-displacement data. From the test data, the energy absorbed by each specimen was obtained, and the *J*-integral was determined using Eq.(1). However, this approach has obvious disadvantages: multiple specimens must be tested and experimental analysis is

very complicated. Thus, a simple experimental technique was sought for estimating the *J*-integral from a single specimen test.

Among others, the most notable was the analysis of Rice *et al*.(1973), who showed that it was easier to determine the *J*-integral directly from the load-displacement curve for a single specimen by using an approximate formula. Among different fracture specimens, only SENB specimens and CT specimens in mode-I opening loading are discussed in this review. Fig.1 shows schematically the geometry sizes and configurations for SENB and CT specimens, where *W* is the specimen width, *a* is the crack length, *S* is the beam span of SENB specimen, and *H* is the height of CT specimen. For convenience, Rice *et al*.(1973) introduced two alternative but equivalent expressions for the *J*-integral in the following forms:

$$J=\frac{1}{B}\int_0^P\frac{\partial \Delta}{\partial a}\mathrm{d}P, \tag{2a}$$

or

$$J=-\frac{1}{B}\int_0^\Delta\frac{\partial P}{\partial a}\mathrm{d}\Delta, \tag{2b}$$

where *P* is a total generalized load and $\Delta$ is the associated load-point or LLD. For deeply cracked SENB specimens, the *J*-integral was found to be a function of the work done to the cracked body, and Eq.(2) was simplified as

$$J=\frac{2}{Bb}\int_0^\Delta P\mathrm{d}\Delta=\frac{2A}{Bb}, \tag{3}$$

where $b=W-a$ is the remaining ligament, *W* is the specimen width, and *A* is the total area under a load-displacement *P*-$\Delta$ curve and represents the work done or the energy absorbed by the specimen as a result of the presence of a crack.

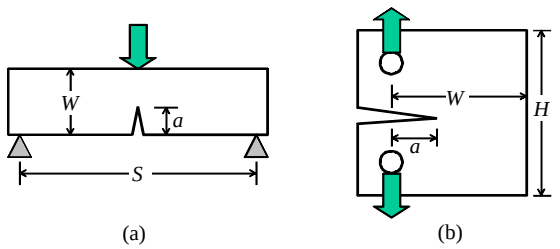


(a) (b)

**Fig.1 Schematic fracture testing specimen geometries. (a) Single edge notched bend (SENB) specimen; (b) Compact tension (CT) specimen**

The simple relationship in Eq.(3) marked a major step forward in the history of the development of a practical method for *J*-integral testing. Eq.(3) was developed initially for deeply cracked SENB specimens in pure bending, where the generalized load was an applied bending moment *M*, and the load-point displacement was a relative rotation $\theta$ at the beam ends. Landes *et al*.(1979) demonstrated that Eq.(3) was also applicable with reasonable accuracy to SENB specimens in three-point bending and CT specimens with deep cracks. This is because their remaining ligaments support primarily a bending moment produced by the applied loads. For determining the best approximation to *J* for CT specimens, Merkle and Corten (1974) proposed a modification of Eq.(3) in a complicated two-term expression, which takes into account the tensile component of the applied load. Among other approximations, Landes *et al*.(1979) proposed the following simplified expression of *J* for CT specimens with $a/W>0.5$:

$$J=\left(\frac{1+\alpha}{1+\alpha^2}\right)\frac{2A}{Bb}, \tag{4}$$

where the parameter $\alpha=2\sqrt{\left(\frac{a}{b}\right)^2+\frac{a}{b}+\frac{1}{2}}-2\left(\frac{a}{b}+\frac{1}{2}\right)$. Eq.(4) indicates that the *J*-integral for CT specimens can be estimated similarly from the energy absorbed by the specimen that is quantified by the total area under the load-displacement curve.

A more general relationship of the *J*-integral estimate that is applicable to different specimen configurations can be written from Eqs.(3) and (4) as follows:

$$J=\frac{\eta}{Bb}\int_0^\Delta P\mathrm{d}\Delta=\frac{\eta A}{Bb}, \tag{5}$$

where $\eta$ is a dimensionless geometry factor that is a function of crack length to specimen width ratio, $a/W$ only. When $\eta=2$, Eq.(5) reduces to Eq.(3) for deeply cracked SENB specimens, and when $\eta=2(1+\alpha)/(1+\alpha^2)$, Eq.(5) reduces to Eq.(4) for deeply cracked CT specimens. Eq.(5) expresses the *J*-integral generally as the energy absorbed by a fracture specimen, divided by the cross-sectional area, times a geometry factor.

The use of the $\eta$ factor considerably simplifies the task of $J$-integral determination, and Eq.(5) gives a very convenient way to evaluate $J$ experimentally for any fracture specimen from a single load-displacement record, provided that the $\eta$ factor is determined priori for that specimen. For CT specimens with deep cracks, Clarke and Landes (1979) proposed an approximate expression for the $\eta$ factor as

$$\eta=2+0.522b/W. \tag{6}$$

In reference to the limit load analysis for SENB specimens in pure bending, Sumpter (1987) obtained the $\eta$ factor for a complete range of crack sizes as

$$\eta=\begin{cases}2, & a/W>0.282;\\ 0.32+12(a/W)-49.5(a/W)^2+99.8(a/W)^3, & a/W\le 0.282.\end{cases} \tag{7}$$

The values of $\eta$ factors in Eqs.(6) and (7) for deeply cracked CT and SENB specimens were adopted by standard ASTM E1820 and all previous versions.

For convenience, a total load-line displacement is often separated into an elastic and a plastic component, i.e., $\Delta=\Delta_{el}+\Delta_{pl}$. At any loading point, the elastic component of LLD can be calculated as the load times the elastic load-line compliance, i.e., $\Delta_{el}=C_{LLD}P$, and the plastic component is the total displacement less the elastic displacement. From this displacement relationship and using Eq.(2b), the total $J$-integral can be separated similarly into elastic and plastic components

$$J=J_{el}+J_{pl}, \tag{8}$$

where the elastic $J$ can be directly and accurately calculated from the stress intensity factor $K$, as used in ASTM E1820 for plane strain mode-I cracks:

$$J_{el}=K^2(1-\nu^2)/E, \tag{9}$$

where $E$ is Young's modulus and $\nu$ is Poisson's ratio. The solutions of the stress intensity factor and elastic compliance for many fracture specimens were compiled in a handbook by Tada *et al*.(1973). Eq.(9) is often used to convert the plane strain fracture toughness between $K_{IC}$ and $J_{IC}$. Note that the elastic $J$ can also be expressed similarly in Eq.(5) with the elastic $\eta$ factor determined from the elastic compliance of a specimen (Turner, 1973). Apparently, the use of Eq.(9) is much simpler and more accurate when the elastic $J$-integral calculation is needed.

Since the elastic $J$ can be accurately obtained from Eq.(9), the determination of total $J$ becomes the task of plastic $J$ calculation. Sumpter and Turner (1976) found that the relationships in Eqs.(2a), (2b) and (5) for a total $J$ are applicable to plastic $J$ in terms of load and plastic displacement data:

$$J_{pl}=\frac{1}{B}\int_0^P\frac{\partial\Delta_{pl}}{\partial a}\mathrm{d}P, \tag{10a}$$

$$J_{pl}=-\frac{1}{B}\int_0^{\Delta_{pl}}\frac{\partial P}{\partial a}\mathrm{d}\Delta_{pl}, \tag{10b}$$

$$J_{pl}=\frac{\eta A_{pl}}{Bb}, \tag{11}$$

where the plastic geometry factor $\eta$ is a function of $a/W$ and independent of loading, and $A_{pl}$ denotes the area under the $P$-$\Delta_{pl}$ curve. For CT and SENB specimens, the plastic $\eta$ factor has the same expressions in Eqs.(6) and (7). Detailed discussions on the plastic $\eta$ factor were given by Paris *et al*.(1980), who pointed out that the concept of expressing $J$ as a function of $A_{pl}$ and $\eta$ plastic factor is rigorous only when the variables of geometry and degree of deformation are separable. Fortunately, about ten years later, Sharobeam and Landes (1991; 1993) strictly verified the existence of a load separation relationship for ductile materials using detailed experimental and numerical analyses. This laid a solid foundation for the simple $J$-integral estimate using the $\eta$ factor equation approach. Eqs.(8), (9) and (11) were used in the basic procedure in ASTM E1820 for the evaluation of initiation toughness, $J_{IC}$, where a full range of crack growth resistance curve is not required.

**$J$-integral estimates for growing cracks**

All equations introduced above are valid only for stationary cracks in the determination of the $J$-integral and its critical value at fracture initiation. However, the early $J$-$R$ curves were constructed simply by using the $J$-integral that was calculated by Eq.(5) in terms of the original crack size and crack extension that was measured using an unloading compliance technology

(Clarke *et al*., 1976). The resulting value tends to overestimate $J$ for a growing crack because the crack growth correction was not taken into account. To allow for crack growth, Eqs.(5) and (11) have been extended in different ways, and several approaches were then developed to obtain a crack growth corrected $J$ as needed in an accurate $J$-$R$ curve evaluation. Two examples are incremental equations, where test data are spaced at small intervals of crack extension and the $J$-integral is evaluated always from the previous step. The first incremental equation for the $J$-integral estimate was proposed by Garwood *et al*.(1975) for a single edge bending specimen with a deep crack. At the $n$th step of crack growth, the total $J$ was determined as

$$J_n = J_{n-1}\left(\frac{W-a_n}{W-a_{n-1}}\right)+\frac{2U_4}{B(W-a_{n-1})}, \tag{12}$$

where the variable $U_4$ refers to the increment of the total area under an actual load-displacement record from step $n-1$ to $n$. Etemad and Turner (1985) and Etemad *et al*.(1988) generalized Eq.(12) for an arbitrary fracture specimen in the form of

$$J_n = J_{n-1}\left(1+\frac{g(\eta)_n}{(W-a_n)}(a_n-a_{n-1})\right)+\frac{\eta_n \Delta U_{n,(n-1)}}{B(W-a_n)}, \tag{13}$$

where $g(\eta)$ is another geometry factor related to the plastic $\eta$ factor by

$$g(\eta)=1+\frac{b}{\eta}\frac{\mathrm{d}\eta}{\mathrm{d}a}-\eta. \tag{14}$$

The second incremental equation for the $J$-integral estimate was obtained by Ernst *et al*.(1981) based on the principle of variable separation. Since the $J$-integral was developed on the basis of the deformation theory of plasticity, it was shown that $J$ is independent of the loading path leading to the current values of load-line displacement and crack size, provided that the $J$-controlled crack growth conditions proposed by Hutchinson and Paris (1979) are satisfied. As a result, the deformation theory based $J$-integral is a unique function of two independent variables: load-line displacement, $\Delta$ and crack length, $a$. From Eq.(5), Ernst *et al*.(1981) derived a complete differential of the total $J$-integral in the form of

$$\mathrm{d}J=\frac{\eta}{bB}P\mathrm{d}\Delta-\frac{\gamma}{b}J\mathrm{d}a, \tag{15}$$

where $\gamma$ is a geometry factor related to the plastic $\eta$ factor by

$$\gamma=\eta-1-\frac{b}{W}\frac{\eta'}{\eta}, \tag{16}$$

where the prime denotes the partial differential with respect to $a/W$, i.e., $\eta'=\dfrac{\partial\eta}{\partial(a/W)}$. Eqs.(14) and (16) show that $g(\eta)=-\gamma$, and these two geometry factors are used to take into account the crack growth correction on $J$. Integrating Eq.(15) gives

$$J=\int_0^{\Delta}\frac{\eta}{bB}P\mathrm{d}\Delta-\int_{a_0}^{a}\frac{\gamma}{b}J\mathrm{d}a. \tag{17}$$

This equation holds for any loading path leading to the current values of $a$ and $\Delta$, including the actual loading path for a growing crack. Fig.2 illustrates a typical $P$-$\Delta$ curve for a growing crack and includes three deformation paths: one for the original crack length $a_0$, and the other two for arbitrarily fixed crack lengths $a_{i-1}$ and $a_i$. As $J$ in Eq.(17) is valid for any loading path leading to the current values of $a_i$ and $\Delta_i$, the integration path $AC$ can be approximated by the deformation segment $AB$ with the fixed crack length $a_{i-1}$ and the segment $BC$ where the displacement $\Delta_i$ remains constant, but the crack size jumps from $a_{i-1}$ to $a_i$. Along the segments $AB$ and $BC$, the total $J$ at the $i$th step of crack growth was determined as

$$J_i=\left(J_{i-1}+\frac{\eta_{i-1}}{Bb_{i-1}}A_{i-1,i}\right)\left(1-\frac{\gamma_{i-1}}{b_{i-1}}(a_i-a_{i-1})\right), \tag{18}$$

where $A_{i-1,i}$ is the incremental area under an actual load-displacement record from step $i-1$ to $i$. Both incremental equations in Eqs.(13) and (18) consider the crack growth correction on the $J$-integral from the last step. Eq.(18) also makes the correction on the incremental work done to the specimen, but Eq.(13)

does not. As a result, a larger $J$ estimate is likely to be obtained from Eq.(13) than from Eq.(18), as shown by test data in Ernst *et al*.(1981). In general, these two typical incremental formations of the $J$-integral equation are applicable to any specimens, provided that the two geometry factors are known for each specimen.

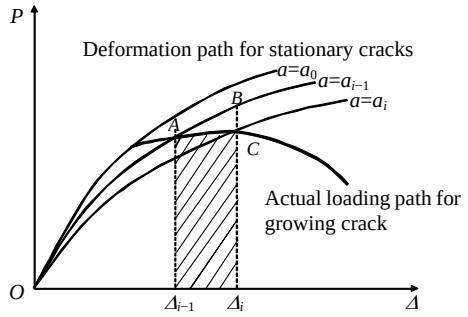


**Fig.2 Typical load vs load-line displacement curves for static and growing cracks**

Anderson (1995) proposed another incremental equation with a different derivation:

$$J_2 = J_1\left(1-\frac{\gamma_1}{b_1}(a_2-a_1)\right)+\frac{\eta_2 P_2(\Delta_2-\Delta_1)}{B_N b_2}, \quad (19)$$

where the subscripts 1 and 2 denote the previous and current load steps, respectively, and $B_N$ is net thickness. Eq.(19) is similar to Eq.(13) for the $J$ estimate.

In ASTM E1820, the total $J$-integral is split into elastic and plastic parts, as shown in Eq.(8), and determined separately. The objective is to improve the accuracy of $J$ estimates, and to obtain consistency of $J$ when near linear elastic conditions are applied. For a set of discrete experimental data, at each step of crack growth, the elastic component of $J$ is obtained directly from the stress intensity factor using Eq.(9). Only the plastic component of $J$ is obtained from the $\eta$ factor method. Following the procedures developed by Ernst *et al*.(1981), Kanninen and Popelar (1985) presented a similar incremental equation for the plastic component of $J$-integral:

$$J_{\mathrm{pl}(i)}=\left(J_{\mathrm{pl}(i-1)}+\frac{\eta_{i-1}}{Bb_{i-1}}A_{\mathrm{pl}}^{i-1,\,i}\right)\left(1-\frac{\gamma_{i-1}}{b_{i-1}}(a_i-a_{i-1})\right), \quad (20)$$

where $A_{\mathrm{pl}}^{i-1,\,i}$ is the increment of plastic area under a load-displacement record from step $i-1$ to $i$:

$$A_{\mathrm{pl}}^{i-1,\,i}=0.5(P_i+P_{i-1})(\Delta_{\mathrm{pl}(i)}-\Delta_{\mathrm{pl}(i-1)}). \quad (21)$$

These two equations were adopted by ASTM E1820, with a net thickness $B_N$ being used for specimens with side grooves in place of the full thickness $B$. Small and uniform crack growth increments are required in Eq.(20) for accurate estimates of $J_{\mathrm{pl}(i)}$. With the calculated $J$ and measured crack extension of $(a_i-a_0)$, where $a_0$ is an original crack length, a $J$-$R$ curve is obtained by applying Eqs.(8), (9) and (20) to successive increments of crack growth from a single test.

## Experimental methods for *J*-*R* curve testing

Experimental test methods and procedures in a valid $J$-$R$ curve evaluation depend on the data required for the $J$-integral calculation and instantaneous crack length determination. Eq.(20) that is used for calculating crack growth corrected $J$-integral requires the simultaneous measurements of load, load-line displacement and crack length. The most commonly used experimental method for a single specimen test is the elastic unloading compliance technique (Clarke *et al*., 1976; Joyce and Gudas, 1979; Joyce, 1992). This method is the ASTM E1820 recommended experimental technique that measures load, LLD and CMOD data for SENB specimens, and determines instantaneous crack length at regular intervals during the test by partially unloading the specimen and measuring CMOD compliance. As the crack grows, the specimen becomes less stiff and the compliance increases. Note that for CT specimens, CMOD gages can be mounted in the load line direction, and thus the LLD and CMOD become identical.

Another conventional experimental technique is a direct current electric potential drop method (Johnson, 1965; Schwalbe and Hellmann, 1981; Bakker, 1985; Marschall *et al*., 1990). This method monitors crack growth through a change in electric resistance which accompanies a loss in the cross sectional area. When a constant current is applied to a specimen, the electrical potential increases as the crack grows. An alternative method for direct determination of crack length is a normalization technique (Joyce, 2001) that is discussed later. References to more detailed experimental techniques and test methods for $J$-$R$ curve testing can be found in an ASTM manual by Joyce (1996).

**CMOD-based *J* estimates for stationary cracks**

Experiments showed that an accurate measurement of LLD is more difficult than that of CMOD for SENB specimens, particularly for shallow cracks. Sumpter (1987) first used load-CMOD data to directly evaluate the values of *J*-integral for bending specimens in an attempt to analyze surface or shallow cracks occurring on welds. Following Sumpter's (1987) basic idea, Kirk and Dodds (1993) investigated several possibilities for estimating *J*-integral for shallowly cracked SENB specimens through use of detailed elastic-plastic finite element analyses (FEA). They found that the LLD-based *J* estimate equation could give inaccurate results for hardening materials because the corresponding plastic $\eta$ factor is very sensitive to the strain hardening exponent for SENB specimens with shallow cracks of $a/W<0.3$. In contrast, for the same geometry, the CMOD-based plastic $\eta$ factor is nearly insensitive to the strain hardening exponent, when a similar $\eta$ factor equation was used with the plastic area being determined under the load-CMOD curve. Thus, Kirk and Dodds (1993) concluded that the CMOD-based *J* estimate is the most reliable and suggested using the following equation to estimate the *J*-integral for SENB specimens with a wide range of crack length:

$$J=\frac{K^2(1-\nu^2)}{E}+\frac{\eta_{\mathrm{CMOD}}A^{\mathrm{pl}}_{\mathrm{CMOD}}}{Bb}, \tag{22}$$

where the CMOD-based plastic geometry factor was determined by fitting their FEA results as

$$\eta_{\mathrm{CMOD}}=3.785-3.101(a/W)+2.018(a/W)^2,\quad 0.5\le a/W\le 0.7. \tag{23}$$

Morrison and Karisallen (1995) and Wang *et al*.(1997) employed these two equations with use of CMOD data in their experimental evaluations of *J*-integral and its critical value $J_{\mathrm{C}}$ for SENB specimens made of different metals. Good agreement was found between the LLD and CMOD based *J*-integral equations, and the benefits of experimental instrumentation using CMOD data were demonstrated. Because of the absence of the corresponding incremental equation, however, the CMOD based *J*-integral equations did not achieve practical application and were not used by the ASTM standard for more than ten years until 2005 when they were adopted in the basic procedure in ASTM E1820-05a.

## RECENT DEVELOPMENTS IN *J*-*R* CURVE TESTING

**More accurate *J*-integral incremental equations**

In the experimental evaluation of *J*-*R* curves, the LLD based *J*-integral incremental Eq.(18) or (20) has been used widely as an 'accurate' expression because it considers crack growth correction and was adopted by ASTM E1820. In contrast, the other two incremental Eqs.(13) and (19) did not receive attention until 2008 when two similar equations were proposed. Based on the jump-like crack growth model, Neimitz (2008) obtained a *J*-integral incremental equation specifically for deeply cracked SENB specimens, and this LLD based equation is similar to Eq.(12). Kroon *et al*.(2008) presented another *J*-integral incremental equation in a general form similar to Eq.(13). These two publications attracted the attention of ASTM E1820 developers, and a question was raised at the ASTM E08.07.05 Task Group Meeting in Denver in 2008: which form of the *J*-integral incremental equations is better or more accurate? To answer this question, Zhu and Joyce (2009a) proposed different mathematical models and physical models in an attempt to determine a more accurate approximation of *J*-integral for a growing crack. Based on the basic ideas developed by Ernst *et al*.(1981), an actual loading path was approximated by multiple segments on different deformation paths (Fig.2). Three physical models: the upper step-line approximation (USLA), lower step-line approximation (LSLA) and median step-line approximation (MSLA) models were developed for *J*-integral estimates. Several approximate formulas were proposed, but only three incremental equations can be classified typically to be independent and are expressed as follows:

(1) For the USLA model,

$$J_{\mathrm{pl}(i)}=\left(J_{\mathrm{pl}(i-1)}+\frac{\eta_{i-1}}{Bb_{i-1}}A^{i-1,\,i}_{\mathrm{pl}}\right)\left(1-\frac{\gamma_{i-1}}{b_{i-1}}(a_i-a_{i-1})\right). \tag{24}$$

The above equation is the same as Eq.(20) and that used by ASTM E1820. For this USLA model, the crack growth correction is considered in the

modification of the previous $J$ value and the incremental work done to the specimen between two loading steps from $i-1$ to $i$.

(2) For the LSLA model,

$$J_{\mathrm{pl}(i)}=J_{\mathrm{pl}(i-1)}\left(1-\frac{\gamma_{i-1}}{b_{i-1}}(a_i-a_{i-1})\right)+\frac{\eta_i}{Bb_i}A_{\mathrm{pl}}^{i-1,\,i}. \tag{25}$$

The above equation is similar to Eq.(13) and the 'new' equations by Neimitz (2008) and Kroon *et al*.(2008). Note that for this LSLA model, the crack growth correction is considered only for the previous $J$ value, but not for the incremental work done to the specimens.

(3) For the (MSLA model,

$$\begin{aligned}J_{\mathrm{pl}(i)}=&J_{\mathrm{pl}(i-1)}\left(1-\frac{\gamma_{i-1}}{b_{i-1}}(a_i-a_{i-1})\right)\\&+\left[\frac{1}{2B}\left(\frac{\eta_{i-1}}{b_{i-1}}+\frac{\eta_i}{b_i}\right)A_{\mathrm{pl}}^{i-1,\,i}\right]\left(1-\frac{\gamma_{i-1}}{2b_{i-1}}(a_i-a_{i-1})\right).\end{aligned} \tag{26}$$

The above equation is a genuinely new one, and equal to the average of Eqs.(24) and (25). In this MSLA model, a full crack growth correction is considered for the previous $J$ value, and a half of the crack growth correction is considered for the incremental work done to the specimen.

The accuracy of these three $J$-integral incremental equations was evaluated in detail using theoretical and experimental results, and presented by Zhu and Joyce (2009a). Fig.3, for example, shows a comparison of the $J$-$R$ curves obtained from Eqs.(24)~(26) with a given $J$-$R$ curve in a theoretical validation approach, where an SENB specimen with $a/W$=0.5 and strain hardening exponent of $n$=0.2 were considered. For the larger crack growth increment equal to 2% of the original crack ligament, i.e., d$a$=0.02$b_0$, Fig.3 shows that (1) the USLA model or Eq.(24), as used by ASTM E1820, produces a lower $J$-$R$ curve than the given one, (2) the LSLA model or Eq.(25) generates a higher $J$-$R$ curve than the given one, and (3) the MSLA model or Eq.(26) determines a $J$-$R$ curve which matches well with the given one. Nevertheless, the comparisons showed that the maximum error generated in Eqs.(24) and (25) is not significant and is less than 2% for the maximum crack extension allowed by ASTM E1820. Moreover, for a smaller increment of crack growth, say d$a$=0.005$b_0$, the difference between these three models diminishes and all incremental equations could give similar results that match well with the given $J$-$R$ curve. Therefore, it was concluded that (1) the newly proposed equation or Eq.(26) is the most accurate and is independent of crack growth increments, (2) the traditional Ernst-type equation or Eq.(24) is always conservative, and so can continue to be used, and (3) the Garwood-type equation or Eq.(25) could be non-conservative, and thus is better not used in $J$-$R$ curve evaluation.

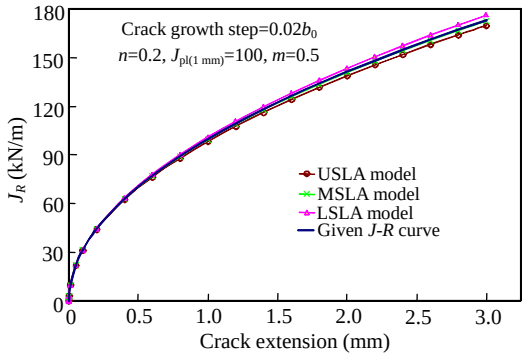


**Fig.3 $J$-$R$ curves determined by three proposed models for high hardening material ($n$=0.2) and the crack growth step size: d$a$=0.02$b_0$**

## Normalization method

The two conventional techniques for online crack size measurements, i.e., the elastic unloading compliance method and the electric potential drop method, are difficult or impractical to implement under severe test conditions, such as high loading rate, high temperature, or aggressive environments. An alternative approach, i.e., the normalization method, was investigated extensively to directly estimate instantaneous crack lengths from load versus load-line displacement data in conjunction with the use of initial and final measurements of physical crack sizes. This method does not require any devices for online monitoring of crack growth, and thus the test costs are reduced. The normalization method was developed based on the principle of load separation (Ernst *et al*., 1981; Sharobeam and Landes, 1991) and the key curve method (Joyce *et al*., 1980). Rather than developing a universal key curve for a given material, this method suggests using an individual calibration curve to determine instantaneous crack length.

Different calibration functions were proposed, including a power-law function (Herrera and Landes, 1988; Joyce, 1992), a combined function of power law and straight line (Herrera and Landes, 1990), and a three-parameter LMN function (Orange, 1990; Landes *et al*., 1991). The LMN function was improved to be a four parameter normalization function by Joyce (2001). Two round-robin test programs were organized by the ASTM E08 Technical Committee for verifying the validity of the normalization method in *J*-*R* curve testing for static loading conditions (Oh *et al*., 2006) and for high-rate loading conditions (Joyce, 2001). It was shown that the normalization method can be equivalent to the elastic compliance method for CT specimens under quasi-static and dynamic loading conditions. The normalization method was accepted by ASTM E1820-01 and its later versions in Annex A15 'Normalization Data Reduction Technique'.

Technically, the normalization method infers crack length change by comparing the measured and normalized load versus load-line displacement data with an analytical normalization function. To obtain a blunting corrected normalization function, measured load data are normalized by the following relationship:

$$P_{\mathrm{N}i}=\frac{P_i}{WB\left(1-\dfrac{a_{\mathrm{b}i}}{W}\right)^{\eta}}, \tag{27}$$

where $i$ refers to the $i$th loading point, $P_{\mathrm{N}i}$ is a normalized load and $a_{\mathrm{b}i}$ is the blunting corrected crack length. From the measured total LLD, $\Delta_i$, a normalized plastic LLD, $\bar{\Delta}_{\mathrm{pl}i}$, is given by

$$\bar{\Delta}_{\mathrm{pl}i}=\frac{\Delta_{\mathrm{pl}i}}{W}=\frac{\Delta_i-P_iC_i}{W}, \tag{28}$$

where $C_i$ is the specimen load-line compliance using the blunting corrected crack length $a_{\mathrm{b}i}$.

Using Eqs.(27) and (28), load-displacement data up to, but not including, the maximum load are normalized. The final load-displacement pair is normalized using the same equations except for the final crack length which is used without blunting correction. From the final normalized point, a tangent line is drawn to the normalized load-displacement curve to define a tangent point. Using the normalized load-displacement pair ($P_{\mathrm{N}i}$, $\bar{\Delta}_{\mathrm{pl}i}$) from $\bar{\Delta}_{\mathrm{pl}i}$>0.001 to the tangent point and the final normalized point, a normalization function can be fitted using the least squares regression in the form of

$$P_{\mathrm{N}}=\frac{c_1+c_2\bar{\Delta}_{\mathrm{pl}}+c_3\bar{\Delta}_{\mathrm{pl}}^2}{c_4+\bar{\Delta}_{\mathrm{pl}}}, \tag{29}$$

where $c_1$, $c_2$, $c_3$ and $c_4$ are the fitting coefficients. With this normalization function, an iterative procedure is further used to force all $P_{\mathrm{N}i}$, $\bar{\Delta}_{\mathrm{pl}i}$ and $a_i$ data at each loading point to lie on the fitted Eq.(29) by adjusting $a_i$. In this way, crack lengths at all data points can be determined.

Following the above procedures, instantaneous crack lengths can be determined, the *J*-integral is calculated from Eqs.(8), (9) and (20), and a *J*-*R* curve is then obtained. For SENB specimens in three-point bending, the applications of this method were demonstrated by Zhu and Joyce (2007) for HY80 steel, Zhu and Leis (2008a) for X80 pipeline steel, and Zhu *et al*.(2009) for A285 carbon steel. All *J*-*R* curves obtained by the normalization method were then compared with those obtained using the unloading compliance method or the electrical potential method. For example, Fig.4a compares the *J*-*R* curves obtained using the normalization methods and the unloading compliance method for a deeply cracked SENB specimen with $a/W$=0.64 in X80 pipeline steel. Fig.4b compares the *J*-*R* curves obtained using the normalization method and the potential drop method for a deeply cracked SENB specimen with $a/W$=0.592 in A285 carbon steel. Fig.4 shows that the three methods agree very well. Along with other validations, this confirms that the normalization method can be equivalent to the unloading compliance method and the potential drop method.

Likewise, Džugan and Viehrig (2004) applied the normalization method to their experimental evaluations of *J*-*R* curves for CT specimens made of various metals, and obtained satisfactory results. Scibetta *et al*.(2006) obtained *J*-*R* curves using the normalization method and load-displacement data determined by FEA, and their 'numerical' *J*-*R* curves match well the experimental results obtained by the unloading compliance method. In addition, the

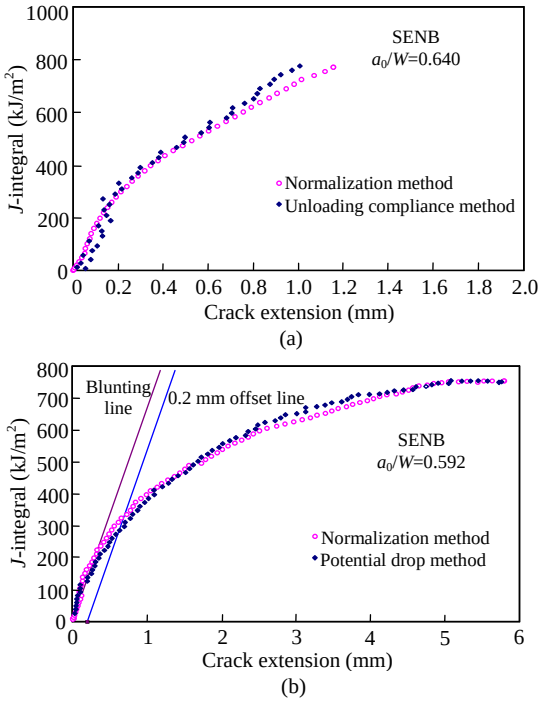


**Fig.4 Comparisons of *J-R* curves obtained by the normalization method with (a) the unloading compliance method for an SENB specimen made of X80 pipeline steel; (b) the potential drop method for an SENB specimen made of A285 carbon steel**

normalization method can be very powerful for evaluating *J-R* curves for non-metallic ductile materials, as demonstrated by Morhain and Velasco (2002) and Joyce and Joyce (2004). However, two points need to be considered carefully when the normalization method is used in a *J-R* curve evaluation. One is the oscillation of the initial *J-R* curve data determined by this method, which can be solved using a blunting line in this area. The other is the difficulty in fitting the four- parameter normalization function for some materials owing to its high nonlinearity. It is a challenge to improve this method and further investigations are needed. In spite of this, the normalization method shows its usefulness in *J-R* curve testing under dynamic loading conditions in comparison with the load ratio method (Hu *et al*., 1992) and the compliance ratio method (Joyce *et al*., 2001). A related review and discussion can be found in (Oh and Hwang, 2006).

## Modified basic method

To unify the different fracture testing standards in Europe and the USA, Wallin and Laukkanen (2004) proposed a new ductile crack growth procedure for *J-R* curve evaluation. This procedure is regarded as an improved basic method of ASTM E1820, and herein is referred to as a modified basic method. In this method, the following four steps are required to determine a crack growth corrected *J-R* curve:

Step 1. Calculate the $J_{\mathrm{el}(i)}(a_0)$ and $J_{\mathrm{pl}(i)}(a_0)$ at a loading point $i$ for an SENB specimen using Eqs.(9) and (11) or (22), respectively. However, when Eq.(22) is used, the $\eta^i_{\mathrm{CMOD}}$ factor should take values in reference to the current crack length $a_i$, rather than to the original crack length $a_0$, as suggested in Wallin and Laukkanen (2004).

Step 2. Determine initial crack growth corrected *J*-integral values for all loading points using the following equation:

$$J_i(\Delta a)=J_{\mathrm{el}(i)}(a_0)+\frac{J_{\mathrm{pl}(i)}(a_0)}{1+\left(\dfrac{\alpha-0.5}{\alpha+0.5}\right)\dfrac{\Delta a}{b_0}}, \tag{30}$$

where $\alpha$=1 for SENB specimens in three-point bending, and $\alpha$=0.9 for CT specimens.

Step 3. Fit a power-law expression of $J=J_{1\,\mathrm{mm}}\Delta a^m$ to the initial crack growth corrected *J-R* curve obtained in Step 2 for crack extension with $\Delta a\geq 0.05b_0$, where $\Delta a=a_i-a_0$, $J_{1\,\mathrm{mm}}$ is the *J*-integral value at 1 mm crack extension and $m$ is an unknown curve-fit parameter.

Step 4. Calculate final crack growth corrected *J*-integral values using the following equation with the curve-fitted $m$ obtained in Step 3:

$$J_i(\Delta a)=J_{\mathrm{el}(i)}(a_0)+\frac{J_{\mathrm{pl}(i)}(a_0)}{1+\left(\dfrac{\alpha-m}{\alpha+m}\right)\dfrac{\Delta a}{b_0}}. \tag{31}$$

Eq.(31) reduces to Eq.(8) when $m=\alpha$. In general, a *J-R* curve approximately follows a power-law curve with $0<m<\alpha$ for most ductile metals, and thus the basic method determines larger *J*-integral values and a higher *J-R* curve than those determined by this modified basic method. The new correction procedures in the modified basic method were developed for standard CT and SENB specimens, and are valid for both LLD and CMOD-based *J*-integral

calculations. They are applicable to both single specimen tests and multiple specimen tests, and have the same or better accuracy as the crack growth correction used in the present ASTM E1820. Therefore, this modified basic method was adopted by ASTM E1820-05 and its later versions in Annex A16 'Evaluation of crack growth corrected *J*-integral values'.

**CMOD-based *J*-integral incremental equations**

CMOD measurements are more accurate than LLD measurements. Thus, a fracture test for SENB specimens favors the use of CMOD gages for measures of displacement and specimen compliance. Using load-CMOD data, a crack growth corrected *J*-*R* curve can be determined using the modified basic method as outlined above. However, the crack growth correction considered in this method is indirect and involves multiple steps in determination of the crack growth corrected *J*-integral for a full-range *J*-*R* curve testing. A direct CMOD method is desirable for determination of a crack growth corrected *J*-*R* curve and is long overdue. To this end, Zhu *et al*.(2008) developed a CMOD-based *J*-integral incremental equation that is similar to the ASTM E1820 LLD-based *J*-integral incremental equation. Based on the deformation theory of plasticity and the energy principle, the *J*-integral was assumed as a function of two independent variables: CMOD and crack length *a*. From the CMOD-based $\eta$ factor Eq.(22), a complete differential of the plastic *J*-integral was obtained in an expression similar to Eq.(15). A CMOD-based $\gamma$ factor is involved, and equal to the LLD-based $\gamma$ factor. Following procedures similar to those of Ernst *et al*.(1981), an actual loading path along the load-CMOD curve was approximated by multiple segments of deformation paths (Fig.2). By integration of this differential equation of *J*-integral along these small segments in one step from loading point $i-1$ to $i$, Zhu *et al*.(2008) obtained a CMOD-based *J*-integral incremental equation in the form of

$$J_{\mathrm{pl}(i)}=\left(J_{\mathrm{pl}(i-1)}+\frac{\eta_{\mathrm{CMOD}}^{i-1}}{b_{i-1}B_{\mathrm{N}}}A_{V_{\mathrm{pl}}}^{i-1,\,i}\right)\left(1-\frac{\gamma_{\mathrm{CMOD}}^{i-1}}{b_{i-1}}(a_i-a_{i-1})\right), \tag{32}$$

for determining the plastic component of the *J*-integral. In this equation, $\eta_{\mathrm{CMOD}}$ and $\gamma_{\mathrm{CMOD}}$ are two CMOD-based plastic geometry factors, $A_{V_{\mathrm{pl}}}^{i-1,\,i}$ denotes the incremental area under the $P$-$V_{\mathrm{pl}}$ curve (where $V_{\mathrm{pl}}$ is the plastic component of measured CMOD), and is calculated by

$$A_{V_{\mathrm{pl}}}^{i-1,\,i}=0.5(P_i+P_{i-1})(V_{\mathrm{pl}}^{i}-V_{\mathrm{pl}}^{i-1}). \tag{33}$$

The elastic component and total value of the *J*-integral are still determined by Eqs.(9) and (8), respectively. Similar to Eq.(20), the $\gamma_{\mathrm{CMOD}}$ term is used for considering the crack growth correction. Note that a similar equation to Eq.(32) was recently proposed by Cravero and Ruggieri (2007) in a different analysis for a single edge notched tension (SENT) specimen. For a special case with equal LLD and CMOD, such as for compact-type specimens where the LLD could be estimated directly from the CMOD gages, the two incremental *J*-integral Eqs.(20) and (32) become identical to each other. In general, Eq.(32) can be used for any specimen, provided that the corresponding geometry factors $\eta_{\mathrm{CMOD}}$ and $\gamma_{\mathrm{CMOD}}$ are known a priori for that specimen.

If Eq.(32) is used for *J*-*R* curve evaluation, the standard test procedures in ASTM E1820 can be simplified considerably, because only load-CMOD data are needed for collection in a test using the elastic unloading compliance method. As a result, if the CMOD direct method is used, *J*-*R* curve testing becomes simpler and more cost-effective, and the results would be more accurate owing to the new *J*-integral formulation and CMOD gages. Therefore, Professor James Joyce, the chief developer of ASTM E1820, was very excited when he saw the CMOD-based *J*-integral incremental equation, and commented that "this relationship has been a long-standing technical gap in ASTM E1820". This CMOD direct method is in the ASTM ballot process for inclusion in ASTM E1820. In addition to this direct CMOD method, Zhu and Leis (2008b) proposed another indirect CMOD method for evaluating a *J*-*R* curve using only load-CMOD data for SENB specimens. They developed a conversion technique to infer LLD data from CMOD measurements and to calculate the *J*-integral still using the LLD-based incremental Eq.(20) in the *J*-*R* curve evaluation.

In the CMOD direct method, the *J*-integral incremental Eq.(32) contains two plastic geometry

factors, i.e., CMOD based $\eta$ and $\gamma$ factors. To use Eq.(32) to calculate the crack growth corrected $J$-integral in a valid $J$-$R$ curve evaluation, these two geometry factors must be known for the tested specimens. The determination of these plastic geometry factors for SENB specimens is of great importance and is discussed next.

**Relationships of $\eta$ and $\gamma$ factors for SENB specimens**

The above analysis indicates that the plastic $\eta$ and $\gamma$ factors have a critical role in an accurate $J$-$R$ curve evaluation. The early methods to determine these geometry factors involved the use of slip-line field (SLF) solutions or limit load solutions, as presented by Clarke and Landes (1979) for CT specimens, Sumpter (1987) for pure bending specimens, and Wu *et al*.(1988; 1990) for various fracture specimens. To consider the effect of the material's work hardening, the elastic-plastic FEA method is the most reliable tool, and is employed widely nowadays to determine the geometry factors (Kirk and Dodds, 1993; Sharobeam and Landes, 1993). For the LLD-based $\eta$ factor in Eq.(7) that was obtained by Sumpter (1987), the resulting expression of the $\gamma$ factor from Eq.(16) was found to have a large jump at $a/W$=0.282. Apparently, the jump is unreasonable, because an appropriate function of the $\eta$ factor should lead to a continuous function of the $\gamma$ factor. Thus, Zhu and Joyce (2007) obtained new expressions for the two geometry factors:

$$\eta=\begin{cases}2, & a/W\geq 0.325;\\ 0.315+8.926(a/W)-11.433(a/W)^2, & a/W<0.325,\end{cases} \tag{34}$$

$$\gamma=\begin{cases}1, & a/W\geq 0.325;\\ -12.769+79.976(a/W)-115.722(a/W)^2, & 0.25<a/W<0.325;\\ 0, & a/W\leq 0.25.\end{cases} \tag{35}$$

Note that these expressions were obtained for SENB specimens in pure bending, and they may be inaccurate for SENB specimens in three-point bending. From the available FEA results of the LLD-based $\eta$ factor for three-point bend specimens, Zhu *et al*.(2008) obtained two curve-fitted functions for LLD-based $\eta$ and $\gamma$ factors as

$$\eta=1.620+0.850(a/W)-0.651(a/W)^2,\ 0.25\leq a/W\leq 0.70, \tag{36}$$

$$\gamma=0.131+2.131(a/W)-1.465(a/W)^2,\ 0.25\leq a/W\leq 0.70. \tag{37}$$

The two expressions above can reduce to those in ASTM E1820-08a for standard SENB specimens with deep cracks:

$$\eta=1.9 \text{ and } \gamma=0.9,\ 0.45\leq a/W\leq 0.70. \tag{38}$$

Extensive FEA indicated that the LLD-based $\eta$ factor is sensitive to the material's strain hardening behavior for three-point bend specimens with very shallow cracks of $a/W$<0.3 (Kirk and Dodds, 1993). Therefore, Eqs.(36) and (37) are not valid for very shallow cracks and further investigations are needed.

In contrast, for the same specimen geometry, the FEA results of the CMOD-based $\eta_{\mathrm{CMOD}}$ are less sensitive to the strain hardening exponent, as demonstrated initially by Kirk and Dodds (1993) and then by Nevalainen and Dodds (1990), Kim *et al*.(2004) and Donato and Ruggieri (2006). However, the comparison of all these available FEA results for $\eta_{\mathrm{CMOD}}$ showed that the FEA results of Kirk and Dodds deviated significantly from the trend formed from other numerical results for deep cracks of $a/W$>0.5. As such, Eq.(23) is acceptable only up to $a/W$=0.5. To correct the errors, Kim and Schwalbe (2001) proposed an alternative solution by fitting the FEA results of Kirk and Dodds for shallow cracks and the SLF solutions of Wu *et al*.(1988) for deep cracks. Recently by fitting all valid FEA results, Zhu *et al*.(2008) obtained an improved, more accurate expression of $\eta_{\mathrm{CMOD}}$ in a quadratic function:

$$\eta_{\mathrm{CMOD}}=3.667-2.119(a/W)+0.437(a/W)^2,\quad 0.05\leq a/W\leq 0.70. \tag{39}$$

This new expression can be used for SENB specimens in three-point bending to cover a full range of crack lengths of interest. Because of its high accuracy, this new expression of $\eta_{\mathrm{CMOD}}$ in Eq.(39) has been adopted in the present version of ASTM E1820-08a. In addition, as proved theoretically by Zhu *et al*.(2008), the resulting CMOD-based $\gamma$ factor is equal to its LLD-based partner. As a result, $\gamma_{\mathrm{CMOD}}=\gamma_{\mathrm{LLD}}=0.9$ for standard SENB specimens with $0.45\leq a/W\leq 0.70$.

With these plastic geometry factors, a *J-R* curve for an SENB specimen can be evaluated by the LLD direct method using the incremental Eq.(20), or by the CMOD direct method using the incremental Eq.(32). Leis *et al*.(2009) employed the CMOD-based *J*-integral incremental Eqs.(32), (39) and (37) and determined *J-R* curves for SENB specimens with cracks from shallow to deep in X80 pipeline steel. Likewise, Zhu and Joyce (2009b) evaluated the CMOD direct method in *J-R* curve determination for SENB specimens with a wide range of crack sizes in HY80 steel. The results of *J-R* curves from the normalization method were compared with those from the CMOD-based basic method, the CMOD-based A16 method, and the LLD-based incremental equation. Fig.5 shows a comparison of *J-R* curves determined by the four different methods for an HY80 SENB specimen with $a_0/W$=0.606. As anticipated, the basic method overestimates the *J-R* curve because the crack growth correction is not considered. The other three methods determine essentially equivalent *J-R* curves for the same specimen. Among these methods, the CMOD direct method is the most theoretically sound, accurate and cost-effective. More practical applications of the CMOD direct method can be expected in *J-R* curve testing and evaluation.

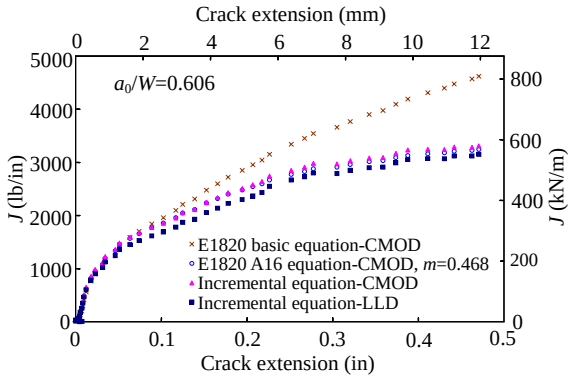


**Fig.5 Comparisons of *J-R* curves determined by the CMOD- and LLD-based equations for an HY80 SENB specimen with $a_0/W$=0.606**

## Constraint-dependent *J-R* curve testing and corrections

Extensive fracture experiments (Hancock *et al*., 1993; Joyce *et al*., 1993; Joyce and Link, 1995; 1997; Lam *et al*., 2003; Neimitz *et al*., 2004; Shen *et al*., 2004) showed that the *J*-integral resistance curves for ductile materials are affected considerably by crack sizes or crack-tip constraint levels under plane strain conditions. Note that the *R* curves are independent of crack sizes for thin sheet materials under plane stress conditions (Schwalbe and Setz, 1981; Reynolds, 1996). If specimens tested have different crack-tip constraints, the measured experimental *J-R* curves are constraint-dependent, with higher curves for low constraint specimens and lower curves for high constraint specimens. SENB specimens with different crack sizes in three-point bending can cover a wide range of crack-tip constraint levels (Joyce and Link, 1997), with higher constraint levels for deep cracks and lower constraint levels for shallow cracks. Therefore, such specimens have been used frequently for determining constraint dependent *J-R* curves for ductile materials, where the guidelines in ASTM E1820 were followed for both standard specimens with deep cracks and non-standard specimens with shallow cracks. Fig.6 shows crack size or constraint-dependent *J-R* curves for SENB specimens with a wide spectrum of crack sizes in HY80 steel that were determined by Zhu and Joyce (2007) using the normalization method. In this figure, the *J-R* curves for HY80 steel increase as the initial crack size becomes shallower, and the deep cracks of $a/W\approx0.5$ give the lowest result. Therefore, ASTM E1820 recommends deeply cracked bending specimens as standard specimens to be used to determine geometry independent, conservative *J*- integral resistance curves for ductile materials.

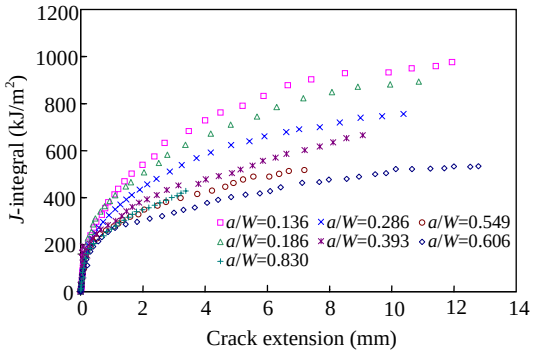


**Fig.6 Experimental *J-R* curves for HY80 SENB specimens with cracks from shallow to deep**

To quantify the crack-tip constraint levels, different fracture constraint theories have been proposed, and many numerical analyses have been performed under both 2D and 3D conditions. Among the

two-parameter elastic-plastic fracture theories, the most notable are the *J*-*Q* theory (O'Dowd and Shih, 1991; 1994) and the *J*-$A_2$ three-term solution (Yang *et al*., 1993; Chao and Zhu, 1998) where *Q* and $A_2$ are constraint parameters. These two theories were developed for power-law hardening materials, and Zhu and Chao (2001) proposed an alternative solution to quantify crack-tip constraint for elastic-perfectly plastic materials. Under large scale yielding conditions, $A_2$ is independent of loading, but *Q* depends on loading. After modifying the *J*-*Q* theory, Zhu *et al*. (2001) proposed a load-independent constraint parameter. For bending specimens like SENB and CT, the global bending moment can significantly impinge on the crack-tip field under large scale yielding. In this situation, as a consequence, both the *J*-*Q* theory and *J*-$A_2$ solution lose the validity to describe the crack-tip field for the bending specimens. To eliminate the global bending influence, a bending modified *J*-*Q* theory was recently proposed by Zhu and Leis (2006b), and a bending modified *J*-$A_2$ solution was proposed by Chao *et al*.(2004). These two modified theories introduced an additional stress term to reflect the global bending influence on the crack-tip field. The results showed that both bending modified asymptotic solutions can well describe the crack-tip field for all deformation levels, and the modified constraint parameters *Q* and $A_2$ are distance- and load-independent under the conditions of large scale yielding.

By using the load-independent constraint parameter *Q* or $A_2$, the present author and his coworkers (Chao and Zhu, 2000; Zhu and Jang, 2000; Lam *et al*., 2003; Zhu and Leis, 2006a and 2006c) have developed a unique methodology for correction of constraint-dependent *J*-*R* curves for a given material. By assuming an analytic power-law function, a family of constraint-dependent *J*-*R* curves can be constructed for ductile crack growth, in conjunction with use of experimental data from at least three typical *J*-*R* curves and numerical results of the constraint parameter values determined by FEA at the loading level of crack initiation toughness. In this way, each experimental *J*-*R* curve is correlated by a fixed value of the constraint parameter used. In general, a constraint-corrected *J*-*R* curve is formulated as a function of the crack extension and the constraint parameter, and can be expressed in a power-law function as

$$J(\Delta a, Q) = C_1(Q)\left(\frac{\Delta a}{1\ \text{mm}}\right)^{C_2(Q)}, \tag{40}$$

if the constraint parameter *Q* is used. A similar expression to Eq.(40) can be assumed if the constraint parameter $A_2$ is used instead of *Q*.

In terms of the constraint parameter *Q*, Zhu and Jang (2000) and Zhu and Leis (2006c) obtained constraint-modified *J*-*R* curves for different ductile metals. For example, Fig.7a shows constraint-dependent *J*-*R* curves for X80 pipeline steel using SENB specimens with different crack sizes, as determined by Zhu and Leis (2006c), where the constraint-corrected *J*-*R* curve is formulated as

$$J(\Delta a,\ Q) = (-1225Q + 645)\left(\frac{\Delta a}{1\,\text{mm}}\right)^{(-0.066Q+0.637)}\ (\text{kJ/m}^2), \tag{41}$$

In reference to the constraint parameter $A_2$, Chao and Zhu (2000), Lam *et al*.(2003) and Zhu and Leis (2006a) obtained constraint-corrected *J*-*R* curves for various ductile materials. Fig.7b shows again the constraint-dependent *J*-*R* curves for the X80 pipeline steel, as determined by Zhu and Leis (2006a), where the constraint-corrected *J*-*R* curve is functioned as

$$J(\Delta a,\ A_2) = -4417.1A_2\left(\frac{\Delta a}{1\ \text{mm}}\right)^{0.668}\ (\text{kJ/m}^2). \tag{42}$$

Fig.7 indicates that *J*-*R* curves predicted by the constraint-corrected *J*-*R* curve function in Eq.(41) or Eq.(42) can match very well the experimental results for X80 pipeline steel that were obtained by Shen *et al*.(2004) using the unloading compliance method and SENB specimens. A similar application and validation of the constraint correction approach in terms of constraint parameters $A_2$ and *Q* was recently presented by Zhou *et al*.(2009) for HY100 steel. Moreover, Chao and Zhu (1998) and Zhu and Chao (2005) showed that the two-parameter *J*-$A_2$ dominant zone at the crack tip is significantly larger than the *J* controlled zone, and the specimen size requirements relax considerably for a valid two-parameter fracture toughness testing. Therefore, it can be concluded that

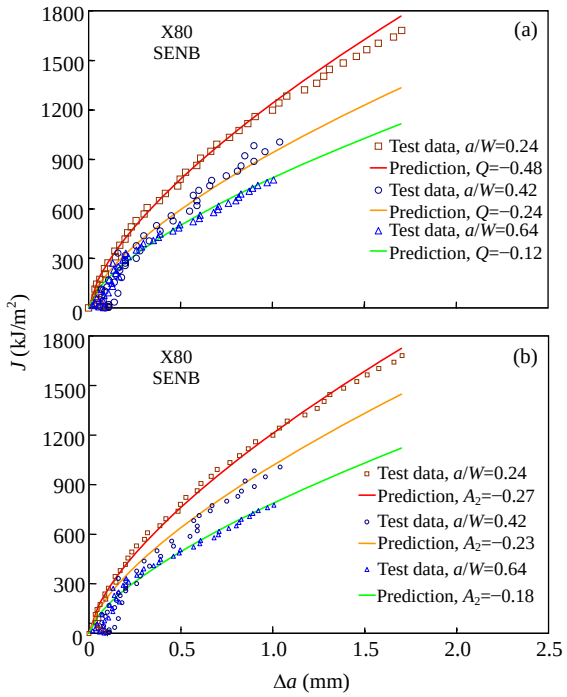


**Fig.7 Comparison of experimental and predicted *J*-*R* curves for X80 SENB specimens with *a*/*W*=0.24, 0.42 and 0.64 using (a) constraint parameter *Q* and (b) constraint parameter $A_2$**

the constraint correction procedures for correlating constraint-dependent *J*-*R* curves are reliable, and the constraint parameters *Q* and $A_2$ are appropriate for use equivalently to determine a family of constraint-corrected *J*-*R* curves for ductile crack growth. More importantly, a constraint-corrected *J*-*R* curve can be used for transferring the laboratory measured fracture resistance curves from small specimens to actual cracked components, provided that the value of the constraint parameter is determined for those components. As a result, this constraint correction technique can effectively correlate size-dependent *J*-*R* curves, reduce unnecessary experimental tests and costs, and serve as a vital tool for solving the transferability issue of fracture toughness in the critical assessment of various ductile materials used in engineering.

## *J*-INTEGRAL RESISTANCE CURVE TEST METHODS IN ASTM E1820-08a

The plane strain fracture toughness test standard ASTM E1820 allows two methods for *J*-integral tests: the basic procedure and the resistance curve procedure. In the basic procedure, the *J*-integral is calculated using the η factor equations as used for stationary cracks. In the resistance curve procedure, the *J*-integral is calculated using the crack growth corrected incremental equations. In the present version of ASTM E1820-08a, several approaches are recommended for calculating the *J*-integral in a fracture toughness test, including the LLD and CMOD-based basic methods, the LLD direct method with use of incremental *J*-integral equations, the A15 normalization method and the A16 modified basic method. An overview of these methods is given in the following paragraphs.

### Basic test method

When a full, crack growth corrected *J* resistance curve is not required, a basic test method is allowed for determining the *J*-integral using load-displacement data and the original crack length $a_0$. For a single specimen test, instantaneous crack sizes are obtained by the unloading compliance method. If multiple specimens are used, the basic procedure involves physical measurements of crack advance. A partial *J*-*R* curve plot is then formed and a single point value of fracture toughness at crack initiation can be evaluated.

The displacement data of LLD or CMOD are allowed to be used in this basic test method. If load-LLD data are used, Eqs.(8), (9) and (11) are used to determine the *J*-integral, and the related η factor takes the value in Eq.(6) for CT specimens and in Eq.(38) for SENB specimens. If load-CMOD data are used for SENB specimens, Eq.(22) is used to determine the *J*-integral, and the related η factor takes the value in Eq.(39). All *J*-integral values obtained by the basic test method shall be corrected for crack growth using the procedure of ASTM E1820 Annex A16. Nevertheless, for a small crack extension, say less than 2 mm, the crack growth correction has a limited effect on a *J*-*R* curve obtained by the basic test method. Note that the basic method is recommended for determining the initiation toughness, not for a full range of resistance curve.

### Resistance curve test method

Only the single specimen test is allowed to be used for developing a full range *J*-*R* curve in the resistance curve test method. The elastic unloading

compliance method is recommended for online monitoring of crack growth. Alternative methods of measuring crack extension, such as the electric potential drop method, are allowed if the qualification criteria are met. The resistance curve test method requires simultaneous measurements of load, LLD, and CMOD data for a single test on SENB specimens. Note that for CT specimens, CMOD gages could be mounted in the load-line direction and thus LLD and CMOD become identical. The load-CMOD data are used to determine compliance-based crack length $a$, while the load-LLD data in conjunction with the crack length are used to calculate the $J$-integral. The elastic component of $J$ is calculated from Eq.(9) using the current crack length, the plastic component of $J$ is calculated incrementally using Eq.(20) with the $\eta$ and $\gamma$ factors taken from Eq.(38), and the total $J$ is obtained by adding its elastic and plastic values in Eq.(8). With the calculated $J$ and measured crack extension, a $J$-$R$ curve is constructed for a single specimen test, and fracture initiation toughness can be then determined by following the procedures in Annex A9.

**Normalization method in Annex A15**

The normalization method is recommended for use in some cases for obtaining a $J$-$R$ curve directly from a load versus load-line displacement record taken with initial and final crack size measurements from the specimen fracture surface. The normalization technique is most valuable for cases where high loading rates are used, or where high temperatures or aggressive environments are being used. In these and other situations, the unloading compliance method is impractical. Eqs.(27) and (28) are used to normalize the test data of load and displacement, and Eq.(29) is used to fit an analytic normalization function and then to iteratively solve instantaneous crack lengths. With the estimated crack lengths and measured load-displacement data, the $J$-integral is incrementally determined using Eq.(20) and then a $J$-$R$ curve is obtained for a single specimen test. Note that the normalization method is not applicable to low toughness materials tested in large specimen sizes where a large amount of crack extension can occur without measurable plastic load-line displacement.

**Modified basic method in Annex A16**

The modified basic method provides an indirect procedure for evaluation of crack growth corrected $J$-$R$ curves. It is applicable to both single and multiple specimen tests with use of LLD or CMOD data. The four steps presented in the section on the modified basic method must be followed, with Eqs.(30) and (31) being used to determine a crack growth corrected $J$-integral in an experimental evaluation of $J$-$R$ curves. Note that this method determines only approximate results which are adequate for multiple specimen tests. If an accurate, full range $J$-$R$ curve is needed, the resistance curve method and single specimen test technique should be employed.

## CONCLUSION

This paper presents a detailed technical review of $J$-integral resistance curve testing and experimental evaluation methods with an emphasis on recent developments. The review describes the history and current state of the art of $J$-$R$ curve testing, and discussed the development and progress of the plane strain fracture toughness test standard ASTM E1820. These cover a wide spectrum of the technology of $J$-$R$ curve testing from the early efforts to recent developments, including the $J$-integral concept and different methodologies for $J$-integral estimates and for $J$-$R$ curve testing. Typical comparisons of $J$-$R$ curves for several ductile steels determined by different test methods were given and showed that the traditional method of LLD-based $J$-integral incremental equations can continue to be used, and the recently proposed CMOD direct method with use of incremental equations is recommended for use in a valid $J$-$R$ curve testing when SENB specimens are employed for test because this method is more cost-effective and more accurate. For dynamic loading and other aggressive conditions, the normalization method would be a practical technology for fracture resistance curve testing. The constraint correction approach is suggested being used when the transferability of fracture toughness is needed in practical application.

This review indicates that the $J$-integral concept and its experimental evaluation analysis for ductile

materials have experienced a long journey of more than 40 years in the development of technology, and significant progress has been achieved. This is demonstrated by the progress of the ASTM fracture toughness test standard that grew step by step from E813, E1152, E1737, E1820, to the present version of E1820-08a. Now the *J*-integral resistance curve test procedures have become more simplified, the test conditions are wider, the *J*-integral experimental estimates are more accurate, the test costs have been reduced, and the test results are more reliable. This progress was achieved owing to the work of many researchers and scientists around the world who have made many contributions to this field. Although a huge number of publications are available, only the most relevant publications were referenced in this work, in conjunction with the most important equations and relationships presented. Remaining challenges and the author's perspectives for further improving *J*-*R* curve testing and evaluation were also provided in the paper.

Note that this paper focuses only on the review of fracture parameter *J*-integral and its experimental testing and evaluation methods. The other fracture mechanics parameters, such as crack-tip opening displacement (CTOD), crack-tip opening angle (CTOA) or stress intensity factor *K*-based *R* curve, may be appropriate for use in some practical applications. Related research and reviews can be found in recent publications by Newman *et al*.(2003) and Zerbst *et al*.(2009). A general review of fracture mechanics theory and its development was presented by Cotterell (2002). Applications of fracture toughness and fracture mechanics methods to comprehensive structural integrity assessment and management in various engineering fields were recently described in detail in a series of books with ten volumes edited by Milne *et al*.(2003).

## References


Anderson, T.L., 1995. Fracture Mechanics: Fundamentals and Applications (2nd Ed.). CRC Press, USA.

ASTM E1820-08a, 2008. Standard Test Method for Measurement of Fracture Toughness. American Society for Testing and Materials (ASTM) International, West Conshohocken, PA, USA.

Bakker, A., 1985. A DC Potential Drop Procedure for Crack Initiation and *R*-Curve Measurements during Ductile Fracture Tests. Elastic-Plastic Fracture Test Methods: The User's Experience, ASTM STP 586, p.394-410.

Begley, J.A., Landes, J.D., 1972. The *J*-Integral as a Fracture Criterion. Fracture Mechanics, ASTM STP 515, p.1-23.

Chao, Y.J., Zhu, X.K., 1998. *J*-$A_2$ characterization of crack-tip fields: extent of *J*-$A_2$ dominance and size requirements. *International Journal of Fracture*, **89**(3):285-307. [doi:10.1023/A:1007487911376]

Chao, Y.J., Zhu, X.K., 2000. Constraint-modified *J*-*R* curves and its applications to ductile crack growth. *International Journal of Fracture*, **106**(2):135-160. [doi:10.1023/A:1007638400006]

Chao, Y.J., Zhu, X.K., Kim, Y., Lam, P.S., Pechersky, M.J., Morgan, M.J., 2004. Characterization of crack-tip field and constraint for bending specimens under large-scale yielding. *International Journal of Fracture*, **127**(3):283-302. [doi:10.1023/B:FRAC.0000036849.12397.6c]

Clarke, G.A., Landes, J.D., 1979. Evaluation of the *J*-integral for the compact specimen. *Journal of Testing and Evaluation*, **7**(5):264-269. [doi:10.1520/JTE10222J]

Clarke, G.A., Andrews, W.R., Paris, P.C., Schmidt, D.W., 1976. Single Specimen Tests for $J_{IC}$ Determination. Mechanics of Crack Growth, ASTM STP 590, p.27-42. [doi:10.1520/STP33937S]

Cotterell, B., 2002. The past, present and future of fracture mechanics. *Engineering Fracture Mechanics*, **69**(5):533-553. [doi:10.1016/S0013-7944(01)00101-1]

Cravero, S., Ruggieri, C., 2007. Further developments in *J* evaluation procedure for growing cracks based on LLD and CMOD data. *International Journal of Fracture*, **148**(4): 387-400. [doi:10.1007/s10704-008-9211-9]

Donato, G.H.B., Ruggieri, C., 2006. Estimation Procedure for *J* and CTOD Fracture Parameters Using Three-Point Bend Specimens. Proceedings of the 6th International Pipeline Conference, Calgary, Canada.

Džugan, J., Viehrig, H.W., 2004. Application of the normalization method for the determination of *J*-*R* curves. *Materials Science and Engineering A*, **387-389**:307-311. [doi:10.1016/j.msea.2004.01.067]

Ernst, H.A., Paris, P.C., Landes, J.D., 1981. Estimations on *J*-Integral and Tearing Modulus *T* from a Single Specimen Test Record. The 13th Conference on Fracture Mechanics, ASTM STP 743, p.476-502.

Etemad, M.R., Turner, C.E., 1985. An experimental investigation of slow stable crack growth using HY130 steel. *Journal of Strain Analysis for Engineering Design*, **20**(4):201-208. [doi:10.1243/03093247V204201]

Etemad, M.R., John, S.J., Turner, C.E., 1988. Elastic-Plastic *R*-Curves for Large Amounts of Crack Growth. The 18th Symposium on Fracture Mechanics, ASTM STP 945, p.986-1004.

Garwood, S.J., Robinson, J.N., Turner, C.E., 1975. The measurement of crack growth resistance curves (*R*-curves) using the *J* integral. *International Journal of Fracture*, **11**(3):528-530.

Hancock, J.W., Reuter, W.G., Parks, D.M., 1993. Constraint and Toughness Parameterized by *T*. Constraint Effects in Fracture, ASTM STP 1171, p.21-40. [doi:10.1520/STP18021S]

Herrera, R., Landes, J.D., 1988. Direct *J-R* curve analysis of fracture toughness test. *Journal of Testing and Evaluation*, **16**(5):427-449. [doi:10.1520/JTE11618J]

Herrera, R., Landes, J.D., 1990. Direct *J-R* Curve Analysis: A Guide to the Methodology. The 21st Symposium on Fracture Mechanics, ASTM STP 1074, p.24-43.

Hu, J.M., Albrecht, P., Joyce, J.A., 1992. Load Ratio Method for Estimating Crack Extension. The 22nd Symposium on Fracture Mechanics, ASTM STP 1131(I), p.880-903.

Hutchinson, J.W., 1968. Singular behavior at the end of a tensile crack in a hardening material. *Journal of the Mechanics and Physics of Solids*, **16**(1):13-31. [doi:10.1016/0022-5096(68)90014-8]

Hutchinson, J.W., Paris, P.C., 1979. Stability Analysis of *J*-Controlled Crack Growth. Elastic-Plastic Fracture, ASTM STP 668, p.37-64.

Johnson, H.H., 1965. Calibrating the electric potential method for studying slow crack growth. *Materials Research and Standards*, **5**(9):442-445.

Joyce, J.A., 1992. *J*-Resistance Curve Testing of Short Crack Bend Specimens Using Unloading Compliance. The 22nd Symposium on Fracture Mechanics, ASTM STP 1131(I), p.904-924.

Joyce, J.A., 1996. Manual on Elastic-Plastic Fracture: Laboratory Test Procedures. ASTM Manual Series, MNL27, West Conshohocken, PA, USA.

Joyce, J.A., 2001. Analysis of a high rate round robin based on proposed annexes to ASTM E 1820. *Journal of Testing and Evaluation*, **29**(4):329-351. [doi:10.1520/JTE12262J]

Joyce, J.A., Gudas, J.P., 1979. Computer Interactive $J_{IC}$ Testing of Navy Alloys. Elastic-Plastic Fracture, ASTM STP 668, p.451-468.

Joyce, J.A., Link, R.E., 1995. Effects of Constraint on Upper Shelf Fracture Toughness. The 26th Symposium on Fatigue and Fracture Mechanics, ASTM STP 1265, p.142-177.

Joyce, J.A., Link, R.E., 1997. Application of two parameter elastic-plastic fracture mechanics to analysis of structures. *Engineering Fracture Mechanics*, **57**(4):431-446. [doi:10.1016/S0013-7944(97)00030-1]

Joyce, J.A., Joyce, P.J., 2004. Toughness characterization of a metal filled polytetrafluoro-ethylene using the *J*-integral. *Engineering Fracture Mechanics*, **71**(16-17):2513-2531. [doi:10.1016/j.engfracmech.2003.12.009]

Joyce, J.A., Ernst, H., Paris, P.C., 1980. Direct *J-R* Curve Analysis: A Guide to the Methodology. The 12th National Symposium on Fracture Mechanics, ASTM STP 700, p.222-236. [doi:10.1520/STP18031S]

Joyce, J.A., Hackett, E.M., Roe, C., 1993. Effect of Crack Depth and Mode of Loading on the *J-R* Curve Behavior of a High-Strength Steel. Constraint Effects in Fracture, ASTM STP 1171, p.239-263.

Joyce, J.A., Albrecht, P., Tjiang, H.C., Wright, W.J., 2001. Compliance Ratio Method of Estimating Crack Length in Dynamic Fracture Toughness Tests. Fatigue and Fracture Mechanics, ASTM STP 1406, p.139-157.

Kanninen, M.F., Popelar, C.H., 1985. Advanced Fracture Mechanics. Oxford University Press, New York.

Kim, Y.J., Schwalbe, K.H., 2001. On experimental *J* estimation equations based on CMOD for SE(B) specimen. *Journal of Testing and Evaluation*, **29**(1):67-71. [doi:10.1520/JTE12393J]

Kim, Y.J., Kim, J.S., Cho, S.M., Kim, Y.J., 2004. 3-D constraint effects on *J* testing and crack tip constraint in M(T), SE(B), SE(T), C(T) specimens: numerical study. *Engineering Fracture Mechanics*, **71**(9-10):1203-1218. [doi:10.1016/S0013-7944(03)00211-X]

Kirk, M.T., Dodds, R.H., 1993. *J* and CTOD estimation equations for shallow cracks in single edge notch bend specimens. *Journal of Testing and Evaluation*, **21**(4):228-238. [doi:10.1520/JTE11948J]

Kroon, M., Faleskog, J., Oberg, H., 2008. A probabilistic model for cleavage fracture with a length scale—parameter estimation and predictions of growing crack experiments. *Engineering Fracture Mechanics*, **75**(8):2398-2417. [doi:10.1016/j.engfracmech.2007.08.009]

Lam, P.S., Chao, Y.J., Zhu, X.K., Kim, Y., Sindelar, R.L., 2003. Determination of constraint-modified *J-R* curves for carbon steel storage tanks. *Journal of Pressure Vessel Technology*, **125**(2):136-143. [doi:10.1115/1.1564069]

Landes, J.D., Begley, J.A., 1972. The Effect of Specimen Geometry on $J_{IC}$. Fracture Mechanics, ASTM STP 515, p.24-39.

Landes, J.D., Walker, H., Clarke, G.A., 1979. Evaluation of Estimation Procedures Used in *J*-Integral Testing. Elastic-Plastic Fracture, ASTM STP 668, p.266-287.

Landes, J.D., Zhou, Z., Lee, K., Herrera, R., 1991. Normalization method for developing *J-R* curves with the LMN function. *Journal of Testing and Evaluation*, **19**(4):305-311. [doi:10.1520/JTE12574J]

Leis, B.N., Zhu, X.K., Shen, G., Tyson, W.R., 2009. Effective Experimental Measurement and Constraint Quantification of *J-R* Curves for X80 Pipeline Steel. Proceedings of the 12th International Conference on Fracture, Ottawa, Canada.

Marschall, C.W., Held, P.R., Landow, M.P., Mincer, P.N., 1990. Use of the Direct-Current Electric Potential Method to Monitor Large Amounts of Crack Growth in Highly Ductile Metals. The 21st Symposium on Fracture Mechanics, ASTM STP 1074, p.581-593.

Merkle, J.G., Corten, H.T., 1974. A *J* integral analysis for the compact specimen, considering axial force as well as bending effects. *Journal of Pressure Vessel Technology*, **96**(4):286-292.

Milne, I., Ritchie, R.O., Karihaloo, B., 2003. Comprehensive Structural Integrity. Elsevier Science, Amsterdam, Holand.

Morhain, C., Velasco, J.I., 2002. *J-R* curve determination of magnesium hydroxide filled polypropylene using the normalization method. *Journal of Materials Science*, **37**(8):1635-1644. [doi:10.1023/A:1014944729912]

Morrison, J., Karisallen, K.J., 1995. An experimental comparison of *J* and CTOD estimation formulas. *Engineering Fracture Mechanics*, **51**(1):145-149. [doi:10.1016/0013-

7944(94)00239-E]

Neimitz, A., 2008. The jump-like crack growth model, the estimation of fracture energy and $J_R$ curve. *Engineering Fracture Mechanics*, **75**(2):236-252. [doi:10.1016/j.engfracmech.2007.03.020]

Neimitz, A., Dzioba, I., Galkiewicz, J., Molasy, R., 2004. A study of stable crack growth using experimental methods, finite elements and fractography. *Engineering Fracture Mechanics*, **71**(9-10):1325-1355. [doi:10.1016/S0013-7944(03)00169-3]

Nevalainen, M., Dodds, R.H., 1990. Numerical investigation of 3-D constraint effects on brittle fracture in SE(B) and C(T) specimens. *International Journal of Fracture*, **74**(2):131-161. [doi:10.1007/BF00036262]

Newman, J.C., James, M.A., Zerbst, U., 2003. A review of the CTOA/STOD fracture criterion. *International Journal of Fracture*, **70**(3-4):371-385.

O′Dowd, N.P., Shih, C.F., 1991. Family of crack-tip fields characterized by a triaxiality parameter—I. Structure of fields. *Journal of the Mechanics and Physics of Solids*, **39**(8):989-1015. [doi:10.1016/0022-5096(91)90049-T]

O′Dowd, N.P., Shih, C.F., 1994. Two-parameter Fracture Mechanics: Theory and Applications. Fracture Mechanics, ASTM STP 1207, p.21-47.

Oh, Y.J., Hwang, I.S., 2006. Review of dynamic loading *J*-*R* curve method for leak before break of nuclear piping. *Nuclear Engineering and Technology*, **38**(7):639-656.

Oh, Y.J., Hwang, I.S., Joyce, J.A., 2006. Round robin test on normalization method under static loading condition. *Journal of Testing and Evaluation*, **34**(6):537-561.

Orange, T.W., 1990. Methods and Models for *R*-Curve Instability Calculations. The 21st Symposium on Fracture Mechanics, ASTM STP 1074, p.545-559.

Paris, P.C., Ernst, H., Turner, C.E., 1980. A *J*-Integral Approach to the Development of $\eta$ Factors. The 12th Conference on Fracture Mechanics, ASTM STP 700, p.338-251.

Reynolds, A.P., 1996. Comparison of *R*-curve methodologies for ranking the toughness of aluminum alloys. *Journal of Testing and Evaluation*, **24**(6):406-410. [doi:10.1520/JTE11464J]

Rice, J.R., 1968. A path independent integral and the approximate analysis of strain concentration by notches and cracks. *Journal of Applied Mechanics*, **35**(2):379-386.

Rice, J.R., Rosengren, G.F., 1968. Plane strain deformation near a crack tip in a power law hardening material. *Journal of the Mechanics and Physics of Solids*, **16**(1):1-12. [doi:10.1016/0022-5096(68)90013-6]

Rice, J.R., Paris, P.C., Merkle, J.G., 1973. Some Further Results of *J*-Integral Analysis and Estimates. Progress in Flaw Growth and Fracture Toughness Testing, ASTM STP 536, p.231-245.

Schwalbe, K.H., Hellmann, D., 1981. Application of the electrical potential method to crack length measurements using Johnson's formula. *Journal of Testing and Evaluation*, **9**(3):218-221. [doi:10.1520/JTE11560J]

Schwalbe, K.H., Setz, W., 1981. *R* curve and fracture toughness of thin sheet materials. *Journal of Testing and Evaluation*, **9**(4):182-194. [doi:10.1520/JTE11226J]

Scibetta, M., Lucon, E., Schuurmans, J., van Walle, E., 2006. Numerical simulations to support the normalization data reduction technique. *Engineering Fracture Mechanics*, **73**(4):524-534. [doi:10.1016/j.engfracmech.2005.08.009]

Sharobeam, M.H., Landes, J.D., 1991. The load separation criterion and methodology in ductile fracture mechanics. *International Journal of Fracture*, **47**(2):81-104. [doi:10.1007/BF00032571]

Sharobeam, M.H., Landes, J.D., 1993. The load separation and $\eta_{pl}$ development in precracked specimen test records. *International Journal of Fracture*, **59**(3):213-226. [doi:10.1007/BF02555184]

Shen, G., Tyson, W.R., Glover, A., Horsley, D., 2004. Constraint Effects on Linepipe Toughness. Proceedings of the 4th International Conference on Pipeline Technology, Ostend, Belgium, **2**:703-720.

Sumpter, J.D.G., 1987. $J_C$ determination for shallow notch welded bend specimens. *Fatigue and Fracture of Engineering Materials and Structures*, **10**(6):479-493. [doi:10.1111/j.1460-2695.1987.tb00498.x]

Sumpter, J.D.G., Turner, C.E., 1976. Method for Laboratory Determination of $J_C$ (Contour Integral for Fracture Analysis). Cracks and Fracture, ASTM STP 601, p.3-18. [doi:10.1520/STP28634S]

Tada, H., Paris, P.C., Irwin, G.R., 1973. The Stress Analysis of Cracks Handbook. Del Research Corporation, Hellertown, PA, USA.

Turner, C.E., 1973. Fracture toughness and specific energy: a reanalysis of results. *Materials Science and Engineering*, **11**(5):275-282. [doi:10.1016/0025-5416(73)90092-X]

Turner, C.E., 1981. Fracture mechanics assessment and design. *Philosophical Transactions of the Royal Society A: Mathematical Physical and Engineering Sciences*, **299**(1446):73-92. [doi:10.1098/rsta.1981.0010]

Turner, C.E., 1983. Further Development of *J*-Based Design Curve and Its Relationship to Other Procedures. Elastic-Plastic Fracture, ASTM STP 803(II), p.80-102.

Wallin, K., Laukkanen, A., 2004. Improved crack growth corrections for *J*-*R* curve testing. *Engineering Fracture Mechanics*, **71**(11):1601-1614. [doi:10.1016/S0013-7944(03)00165-6]

Wang, Y.Y., Reemsnyder, H.S., Kirk, M.T., 1997. Inference Equations for Fracture Toughness Testing: Numerical Analysis and Experimental Verification. Fatigue and Fracture Mechanics, ASTM STP 1321, p.469-484.

Wu, S.X., Mai, Y.W., Cotterell, B., 1988. Plastic rotation factors of three-point bend and compact tension specimens. *Journal of Testing and Evaluation*, **16**(6):555-557. [doi:10.1520/JTE11276J]

Wu, S.X., Mai, Y.W., Cotterell, B., 1990. Plastic $\eta$-factor of fracture specimens with deep and shallow cracks. *International Journal of Fracture*, **45**(1):1-18. [doi:10.1007/BF00012606]

Yang, S., Chao, Y.J., Sutton, M.A., 1993. Higher-order asymptotic fields in a power-law hardening material.

*Engineering Fracture Mechanics*, **45**(1):1-20. [doi:10.1016/0013-7944(93)90002-A]

Zerbst, U., Heinimann, M., Donne, C.D., Steglich, D., 2009. Fracture and damage mechanics modeling of thin-walled structures—an overview. *Engineering Fracture Mechanics*, **76**(1):5-43. [doi:10.1016/j.engfracmech.2007.10.005]

Zhou, D.W., Xu, W.G., Smith, S.D., 2009. *R*-curve Modeling with Constraint Effect. Proceedings of the 12th International Conference on Fracture, Ottawa, Canada.

Zhu, X.K., Chao, Y.J., 2001. Constraint effects on crack-tip fields in elastic-perfectly plastic materials. *Journal of the Mechanics and Physics of Solids*, **49**(2):363-399. [doi:10.1016/S0022-5096(00)00030-2]

Zhu, X.K., Jang, S.K., 2000. *J-R* curves corrected by load independent parameter in ductile crack growth. *Engineering Fracture Mechanics*, **68**(3):285-301. [doi:10.1016/S0013-7944(00)00100-4]

Zhu, X.K., Chao, Y.J., 2005. Specimen size requirements for two parameter fracture toughness testing. *International Journal of Fracture*, **135**(1-4):117-136. [doi:10.1007/s10704-005-3946-3]

Zhu, X.K., Leis, B.N., 2006a. Application of constraint-corrected *J-R* curve to fracture analysis of pipelines. *Journal of Pressure Vessel Technology*, **128**(4):581- 589. [doi:10.1115/1.2349571]

Zhu, X.K., Leis, B.N., 2006b. Bending modified *J-Q* theory and crack-tip constraint quantification. *International Journal of Fracture*, **141**(1-2):115-134. [doi:10.1007/s10704-006-0068-5]

Zhu, X.K., Leis, B.N., 2006c. Constraint corrected *J-R* curve and its applications for X80 pipeline. *Journal of ASTM International*, **3**(6), paper ID JAI13209. [doi:10.1520/JAI13209]

Zhu, X.K., Joyce, J.A., 2007. *J*-resistance curve testing of HY80 steel using SE(B) specimens and normalization method. *Engineering Fracture Mechanics*, **74**(14):2263-2281. [doi:10.1016/j.engfracmech.2006.10.018]

Zhu, X.K., Leis, B.N., 2008a. Fracture resistance curve testing of X80 pipeline steel using SENB specimen and normalization method. *Journal of Pipeline Engineering*, **7**(2):126-136.

Zhu, X.K., Leis, B.N., 2008b. Experimental Determination of *J-R* Curves Using SENB Specimen and P-CMOD Data. Proceedings of ASME Pressure Vessel and Piping Conference, Chicago, Illinois, USA.

Zhu, X.K., Joyce, J.A., 2009a. More Accurate Approximation of *J*-integral Equation for Evaluating Fracture Resistance Curves. The 9th International ASTM/ESIS Symposium on Fatigue and Fracture Mechanics, Vancouver, Canada.

Zhu, X.K., Joyce, J.A., 2009b. Revised incremental *J*-integral equations for ASTM E1820 using crack mouth opening displacement. *Journal of Testing and Evaluation*, **37**(3):205-214.

Zhu, X.K., Jang, S.K., Chen, Y.F., 2001. A modification of *J-Q* theory and its applications. *International Journal of Fracture*, **111**(3):L47-L52. [doi:10.1023/A:1012424711672]

Zhu, X.K., Leis, B.N., Joyce, J.A., 2008. Experimental evaluation of *J-R* curves from load-CMOD record for SE(B) specimens. *Journal of Pressure Vessels and Piping*, **5**(5), paper ID JAI101532.

Zhu, X.K., Lam, P.S., Chao, Y.J., 2009. Applications of normalization method to experimental measurement of fracture toughness for A285 carbon steel. *Journal of Pressure Vessels and Piping*, **86**(10):669-676. [doi:10.1016/j.ijpvp.2009.03.009]